Detection of heavy metal ions Hg^{2+} and Pb^{2+} based on surface plasmon resonance technique with enhanced sensitivity

Angad Singh Kushwaha[1], Rajeev Kumar[2]

Abstract

In this study, we present a high-performance surface plasmon resonance (SPR)-based metal-ion sensor employing a BK7 glass prism/$BaTiO_3$/gold (Au) hybrid structure. The $BaTiO_3$ layer, characterized by its high real dielectric constant, is strategically incorporated to enhance light–matter interaction at the metal–dielectric interface. Using the angular interrogation method, key sensing performance parameters-sensitivity (S), detection accuracy (DA), quality parameter (QP) and electric field intensity enhancement factor (EFIEF)-are systematically analyzed. The strong dielectric response of $BaTiO_3$, when coupled with the plasmonic properties of gold, significantly improves the confinement of the evanescent field, thereby enhancing the sensing capability of the device. For Hg^{2+} ion detection, the proposed structure demonstrates a sensitivity of 1410 RIU^{-1}, a detection accuracy of 0.178, and a quality parameter of 23.77 RIU^{-1}. In the case of Pb^{2+} ion detection, the achieved sensitivity, detection accuracy, and quality parameter are 1390.43 RIU^{-1}, 0.166, and 23.51 RIU^{-1}, respectively. These values indicate notable improvement over several reported SPR-based metal-ion sensors, highlighting the effectiveness of incorporating $BaTiO_3$ as a functional dielectric layer. Overall, the results confirm that the BK7/$BaTiO_3$/Au hybrid configuration offers enhanced plasmonic field confinement and superior sensing performance, making it a promising candidate for the rapid and highly accurate detection of hazardous metal ions in environmental and biochemical applications.

Keywords: *Surface Plasmon Resonance (SPR), optical sensor, sensitivity, detection accuracy, quality parameter, heavy metal ions.*

Introduction

The heavy metals are elements that have a density above 5 g/cm³. They make up a significant portion of the Earth's crust. These metals are being spread into the environment by the human beings in many ways which is very harmful due to highly toxic nature. The amount of heavy metal ions in the environment is increasing. This is a major problem in many developing countries. It is also a serious issue in developed countries. The most toxic heavy metals are mercury (Hg), cadmium (Cd), lead (Pb), copper (Cu), and zinc (Zn).

In the environment, combustion of fossil fuel produces a large amount of toxic heavy metals which is very dangerous for the living beings. Autonomic dysfunction, the cell division of abnormal central nervous system may occur due to the exposure to mercury. The large amount of exposure to mercury results to coma and also leads to death [1]. Lead that belongs to the family of heavy metals can generate a broad range of repugnant effect in living beings. Premature birth of child, headache, sore muscle, anaemia is observed in the case of low content lead poisoning. Intense poisoning of lead may affect kidney, liver, cardiovascular system, immune system and even leads to death [2-4].

From the study of above paragraph, it is very necessary to recognise these heavy toxic metal ions at early stage. Till now, many detection techniques have been proposed and developed to detect and quantify the trace amount of heavy metal ions. Atomic absorption spectroscopy is a common method for detecting heavy metal ions. X-ray fluorescence spectroscopy is also used for this purpose. Inductively coupled plasma mass spectrometry helps to identify metal ions in samples. Anodic stripping voltammetry is another technique used for detection. These methods are applied to analyze various contaminated samples. These techniques for the detection of are highly sensitive but more expensive, suffer from interference effect and take relatively long span of time [5-8].

Therefore, one of the basic tools to investigate these metal ions is the SPR technique which is very simple and cost effective. There exist many active layers that play the role of recognition elements. Polymers, proteins, and nanoparticles have been used with metals in SPR sensors. They help in the efficient detection of heavy metal ions. The phenomenon of SPR was first observed by Wood [9] in 1902 while studying anomalous diffraction gratings.

OPEN ACCESS

Quick Response Code:

Website: https://wgges.us

Manuscript ID:
IJWGAFES-2025-020907

DOI: 10.5281/zenodo.18213039

DOI Link:
https://doi.org/10.5281/zenodo.18213039

Volume: 2

Issue: 9

September

Year: 2025

E-ISSN: 3066-1552

Submitted: *05 Aug. 2025*

Revised: *10 Aug. 2025*

Accepted: *06 Sept. 2025*

Published: *30 Sept. 2025*

[1]Department of Physics, Dayanand Vedic College, Orai (Jalaun), Uttar Pradesh, India
Email: angad14bhu@gmail.com

[2]Department of Physics, KGK (PG) College, Moradabad, Uttar Pradesh, India

Address for correspondence:
Dr Angad Singh Kushwahaa
Department of Physics, Dayanand Vedic College, Orai (Jalaun), Uttar Pradesh, India
Email: angad14bhu@gmail.com

How to cite this article:
Kushwaha, A. S., & Kumar, R. (2025). Detection of heavy metal ions Hg2+ and Pb2+ based on surface plasmon resonance technique with enhanced sensitivity. International Journal of World Geology, Geography, Agriculture, Forestry and Environment Sciences, 2(9), 30–39.
https://doi.org/10.5281/zenodo.18213039

These anomalies occurred due to the excitation of surface plasmon waves. The modern era of SPR began in 1983 when Liedberg et al. [10] demonstrated its use for sensing applications.

The SPR technique has attracted much attention for detecting heavy metal ions. Modifying the active metal surface with recognition molecules improves the sensor's performance. In 2001, Ock et al. [11] developed an SPR sensor using a squarilium dye (SQ-dye) embedded in a polymeric thin film to detect copper ions. In 2004, Chah et al. [12] proposed a selective optical method for detecting mercuric ions (Hg^{2+}) using 1,6-hexanedithiol (HDT) to modify the sensing surface. They found that HDT on the gold surface enhanced Hg^{2+} adsorption and increased changes in the SPR angle. In a similar manner, several studies have reported the use of SPR for detecting Pb^{2+} ions.

The refractive indices corresponding to different concentrations of heavy metal ions $Hg^{2+}$and Pb^{2+}islisted in Table 1 and Table 2.

Table. 1 The real and imaginary part of refractive index of Hg^{2+} ion for various concentrations [13].

S. No.	Hg^{2+}ion concentration (in ppm)	Real part of refractive index n (±0.0005)	Imaginary part of refractive index k (±0.0002)
1.	0	1.3317	0
2.	0.5	1.3317	0.0002
3.	1	1.3317	0.0002
4.	5	1.3317	0.0003
5.	10	1.3317	0.0005
6.	30	1.3318	0.0010
7.	50	1.3318	0.0014
8.	70	1.3318	0.0021
9.	100	1.3321	0.0029
10.	500	1.3359	0.0061
11.	700	1.3374	0.0071
12.	1000	1.3392	0.0089

Table. 2 The eefractive index values (real and imaginary parts) of Pb^{2+} ions for different concentrations [14].

S. No.	Pb^{2+} ion concentration (in ppm)	Real part of refractive index n (±0.0005)	Imaginary part of refractive index k (±0.0002)
1.	0	1.3317	0
2.	0.5	1.3318	0.0002
3.	1	1.3318	0.0002
4.	5	1.3318	0.0003
5.	10	1.3318	0.0005
6.	30	1.3318	0.0009
7.	50	1.3318	0.0014
8.	70	1.3318	0.0020
9.	100	1.3321	0.0027
10.	500	1.3356	0.0060
11.	700	1.3370	0.0070
12.	1000	1.3388	0.0086

$BaTiO_3$ belongs to the family of pervoskite ferroelectric materials group and shows a large value of electro-optic coefficient. Also, a large value of birefringence (Δn=0.05) arises due to its unique atomic structure [15]. Optical properties of thin film $BaTiO_3$ has widely been studied in different types of electro-optic modulators and waveguides [16,17]. By taking the advantage of $BaTiO_3$ thin films, surface plasmon wave can be modulated at the sensing surface of the sensor [18].

In this work, we studied the performance of an SPR sensor made of $BaTiO_3$ and gold. A thin layer of $BaTiO_3$ is first deposited on the base of a BK-7 prism, followed by a gold layer, as shown in Fig. 1. Deionized (DI) water is used as the sensing medium for heavy metal ions. Numerical analysis shows that the sensitivity, detection accuracy, quality parameter, EFIEF parameter are greatly improved in this sensor. This design can thus be used for the efficient detection of heavy metal ions, including Hg^{2+} and Pb^{2+}, with enhanced sensitivity.

Design consideration and theoretical modeling

1. Configuration of the Proposed SPR Biosensor

The proposed configuration of metal ion SPR biosensor is shown in Fig. 1, and is based on the multilayer structure as shown in Fig. 2.

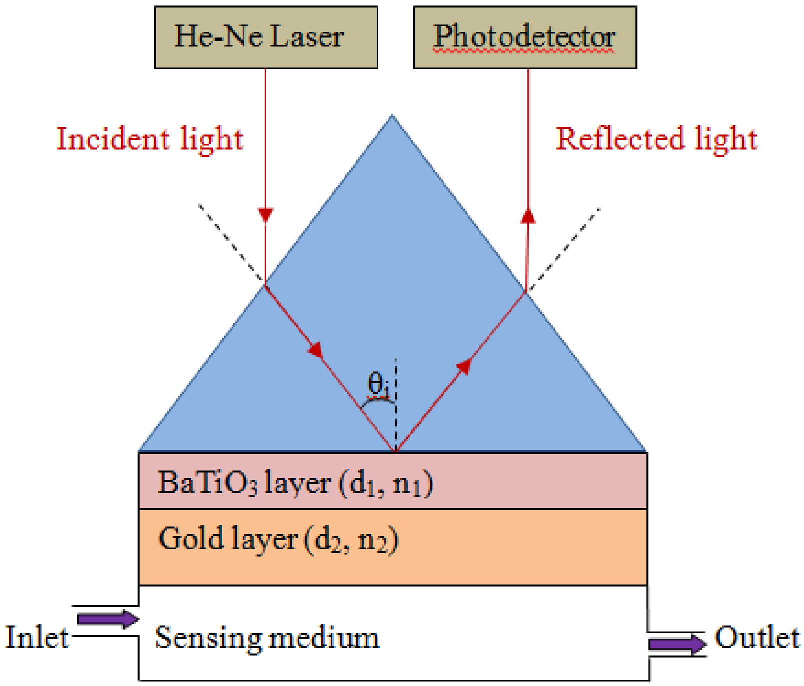

Fig. 1. Proposed configuration: BK-7 prism/$BaTiO_3$/Au and metal ions in sensing medium.

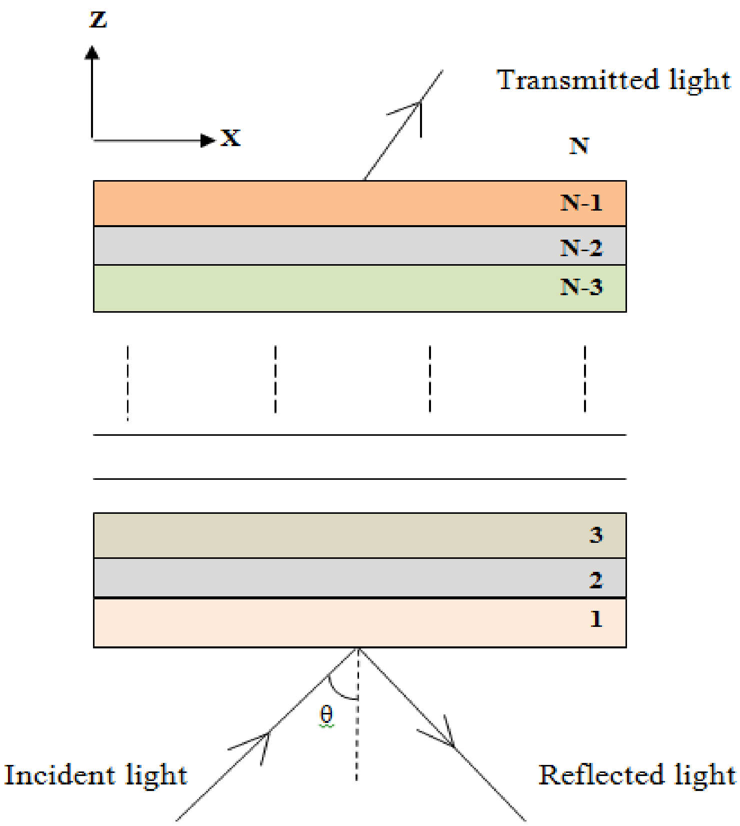

Fig. 2. Schematic diagram of multilayer structure

The proposed SPR biosensor has a planar, multilayer structure consisting of a BK-7 prism, a $BaTiO_3$ layer, a gold (Au) layer, and the sensing medium. The thicknesses of the $BaTiO_3$ and Au layers are optimized to ensure efficient excitation of surface plasmons. In this study, the angular interrogation method is used to evaluate the sensor's performance. The working principle of the SPR biosensor is based on the interaction of the incident light with the metal–dielectric interface, which leads to a resonance condition sensitive to changes in the refractive index of the sensing medium.

$$\frac{\omega}{c}\sqrt{\varepsilon_0}\,\sin\theta_{res} = \frac{\omega}{c}\sqrt{\varepsilon_1\varepsilon_2/(\varepsilon_1+\varepsilon_2)} \quad (1)$$

where ε_0 represents the dielectric constant of the prism, ε_1 is the dielectric constant of the metal and ε_2 denotes the dielectric constant of the sensing medium. The sensing medium can vary according to the application. It may include water, PBS solution, glucose, blood serum, urine, DNA, different proteins, or metal ion solutions of varying concentrations. This versatility makes the SPR sensor suitable for detecting a wide range of chemical and biological analytes.

It is evident from Eq. (1) that any change in the refractive index of the sensing medium alters the resonance condition, as illustrated in Fig. 4 to Fig.7. An increase in the resonance angle shift corresponds to a higher sensitivity of the SPR biosensor. This forms the fundamental sensing principle of SPR-based biosensors [20, 21].

To evaluate the performance of the SPR metal-ion sensor, a BK-7 prism is coated with a high-index dielectric layer of $BaTiO_3$ with a thickness of 22 nm, followed by a gold layer of 42 nm, as shown in Fig. 1. The sensing medium, deionized (DI) water containing metal ions, is placed in close contact with the gold layer. This configuration allows efficient excitation of surface plasmons and enables sensitive detection of heavy metal ions.

In this way, the proposed SPR configuration consists of two nanolayers, $BaTiO_3$ and Au, as shown in Fig. 1. The thickness of the gold layer has been optimized for better performance. To excite surface plasmons, a He–Ne laser with a wavelength of 632.8 nm is directed onto the layered structure at an angle beyond the critical angle of the BK-7 prism. The incident light is reflected from the layered structure on the opposite face of the prism. A photodetector, positioned on this face, collects the reflected light, as illustrated in Fig. 1. The reflected spectra have been recorded and analysed. The sensitivity of the proposed metal ion sensor is calculated by taking the data from reflected spectra.

Table. 3 The refractive indices of used materials in the proposed structure at 632.8 nm wavelength.

Materials used in the proposed structure	Refractive index	Thickness of layers
Prism (BK-7 glass)	1.515	0 nm
Barium Titanate ($BaTiO_3$)	2.411	22 nm
Gold (Au)	0.1838+3.4313i	42 nm

2. Mathematical Formulation of Reflectivity:

We applied the transfer matrix method (TMM) to an N-layer generalized structure to investigate the performance parameters of the proposed SPR sensor [21, 23]. The multilayer arrangement is considered along the Z-axis, as depicted in Fig. 2. The tangential components of the electric field ($E_{0/1}$) and magnetic field ($H_{0/1}$) at the interface of the first layer are connected to those at the interface of the final layer $E_{N/N-1}$ and $H_{N/N-1}$ via the following matrix relation. This method provides an effective way to compute reflectivity and analyze the sensor's key characteristics.

$$\begin{bmatrix} E_{0/1} \\ H_{0/1} \end{bmatrix} = M \begin{bmatrix} E_{N/N-1} \\ H_{N/N-1} \end{bmatrix} \quad (2)$$

In this expression, (M) represents the characteristic matrix of the overall biosensor configuration and can be written as the multiplication of the matrices corresponding to each individual layer,

$$M = \begin{bmatrix} m_{11} & m_{12} \\ m_{21} & m_{22} \end{bmatrix} = \prod_{j=2}^{N-1} M_j \quad (3)$$

$$\text{with } M_j = \begin{bmatrix} \cos\beta_j & \frac{-i}{p_j}\sin\beta_j \\ -ip_j\sin\beta_j & \cos\beta_j \end{bmatrix} \quad (4)$$

In this case, j, β_j and p_j refer to the layer number, the phase thickness, and the transverse refractive index of the respective layer, which can be expressed using the following equations.

$$\beta_j = \frac{2\pi d_j}{\lambda_0}\sqrt{(\epsilon_j - n_0^2\sin^2\theta_0)} \quad (5)$$

$$p_j = \sqrt{(\epsilon_j - n_0^2\sin^2\theta_0)/\epsilon_j} \quad (6)$$

Here, λ_0 is the free-space wavelength, and θ_0 is the incident angle at the base of the prism.
The reflection coefficient of amplitude for TM-polarized incident light is given by

$$r = \frac{(m_{11}+m_{12}p_N)p_1 - (m_{21}+m_{22}p_N)}{(m_{11}+m_{12}p_N)p_1 + (m_{21}+m_{22}p_N)} \quad (7)$$

Now, the overall reflectance ((R)) of the multilayer structure can be determined from the following expression:

$$R = |r|^2 \quad (8)$$

To determine the resonance angle (θ_{res}), the reflectance of the two-layer configuration is plotted against the incident angle (θ_0).The resonance angle (θ_{res}) is identified as the position of the sharp dip in the reflectance spectrum.

3. Performance parameters of SPR biosensor

3.1- The sensitivity (S) of the SPR biosensor configuration is given by the following formula,

$$S = \Delta\theta/\Delta n \quad (9)$$

where, Δn represents the change in the refractive index of the sensing medium due to the adsorption of heavy metal ions on the gold sensing surface, and $\Delta\theta$ denotes the corresponding change in the resonance angle.

3.2- For p-polarized light, the electric or magnetic field enhancement factor (EF) is defined as the ratio of the squared field at the gold–analyte interface to that at the prism–$BaTiO_3$ interface. Specifically, it is the ratio of the square of field $H(N/N-1)$ or $E(N/N-1)$ at the metal–sensing layer boundary to $E(1/2)$ or $H(1/2)$ at the prism–dielectric interface [21]. This parameter quantifies how much the electromagnetic field is intensified at the sensing surface, which is critical for improving the sensitivity and performance of the SPR biosensor. The following relation is-

$$\left|\frac{E\left(\frac{N}{N-1}\right)}{E\left(\frac{1}{2}\right)}\right|^2 = \frac{\varepsilon_1}{\varepsilon_N}\left|\frac{H\left(\frac{N}{N-1}\right)}{H\left(\frac{1}{2}\right)}\right|^2 = \frac{\varepsilon_1}{\varepsilon_N}|t|^2 \tag{10}$$

In this expression, ε_1 and ε_N denote the dielectric constants of the first and N-th layers, respectively, as shown in Fig. 2, and t is the transmission coefficient.

3.3- The detection accuracy of the SPR sensor is determined using the following mathematical expression-

$$SNR = \Delta\theta res/\Delta\theta_{0.5} \tag{11}$$

where $\Delta\theta_{0.5}$ is the spectral width of the SPR spectra at half of the minima.

3.4- The quality factor (Q) of the SPR biosensor is calculated using the following equation-

$$Q = S/\Delta\theta_{0.5} \tag{12}$$

The value of Q strongly depends on the sensitivity and the spectral width of the reflectivity spectra.

Results and discussions:

Fig. 1 shows the layout of the proposed SPR sensor designed for detecting heavy metal ions. In this structure, a $BaTiO_3$ layer is first coated on the base surface of the BK-7 prism, followed by the deposition of a gold layer. Deionized water is used as the sensing medium containing the target metal ions. A He–Ne laser with a wavelength of 632.8 nm is directed onto the prism base from one side, and the reflected beam is collected from the opposite face.

Fig. 2 is the schematic representation of multilayer structure of N-th layers. An incident light beam interacting with the multilayer structure splits into reflected and transmitted components, with the latter reaching the final layer. Fig. 3 depicts the thickness optimization of gold layer that is to be deposited for the proposed SPR biosensor.

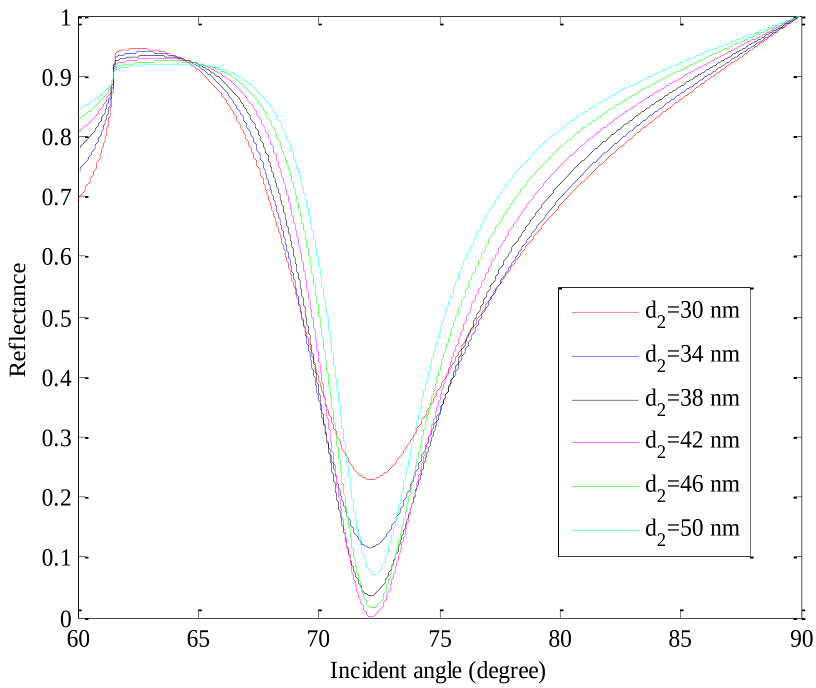

Fig. 3. The thickness optimization of gold layer that is to be deposited for the proposed SPR biosensor.

From Fig. 3, it is obvious that as the thickness (d_2) of gold layer is varied from 30 nm to 50 nm, a sharp dip in reflectance minima occurs at 42 nm. This represents the suitable condition of resonant excitation of SPs which suggests the optimized thickness of Au layer to be 42 nm. When the parallel component of the incident light's wave vector becomes equal to the wave vector of the surface plasmons, resonance takes place. At this point, the incident light transfers most of its energy to the SPs, resulting in a sharp drop in the reflectance curve. This dip is a key indicator of the SPR condition.

Using the optimized 42 nm gold layer, the reflectivity curves are plotted for various concentrations of Hg^{2+} ions. The results, shown in Fig. 4, illustrate how resonance shifts with increasing ion concentration. The refractive index of Hg^{2+} and Pb^{2+} metal ions of different concentration are taken from reference [13,14] and is tabulated in Table 1 and 2 respectively. Fig. 4 and Fig. 5 have been plotted by taking the refractive indices of Hg^{2+} metal ions corresponding to different concentrations i.e. 0 ppm to 1000 ppm.

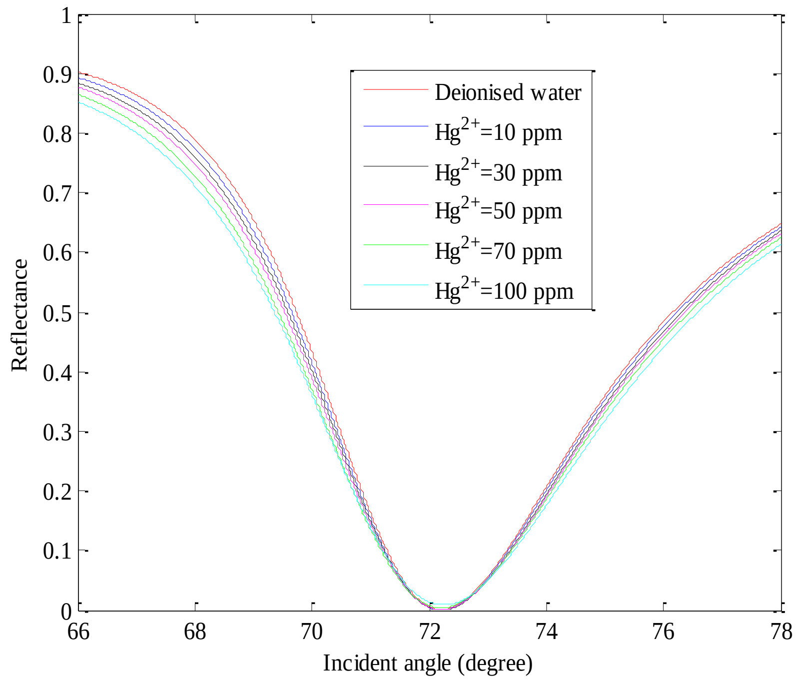

Fig. 4. At optimized thickness of Au, the reflectivity curve is plotted for different concentration 0 to 100 ppm of Hg^{2+} metal ion.

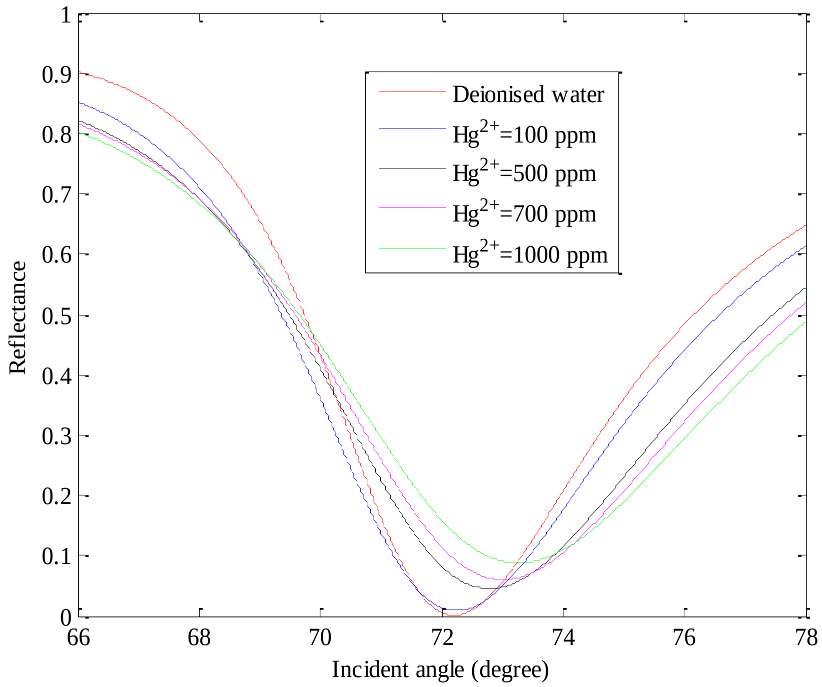

Fig. 5. At optimized thickness of Au, the reflectivity curve is plotted for different concentration 100 to 1000 ppm of Hg^{2+} metal ion.

From Fig. 4, it is evident that the resonance angle variation is zero for very low concentration of Hg^{2+}ions (i.e. below the level of 100 ppm). The existence of small number of ions in low concentrations leads to the similar value of real part of refractive index and due to this reason, the change in resonance angle results to zero value. Now as the refractive index corresponding to different concentrations of Hg^{2+} ions change significantly, a clear change in resonance angle is observed. The resonance angle corresponding to concentrations 0 ppm (DI water), 100 ppm, 500 ppm, 700 ppm and 1000 ppm occur at 72.22^0, 72.25^0, 72.80^0, 73.02^0 and 73.28^0 respectively. From Fig. 5 and using Eq. (9), the calculated sensitivity is 1410 RIU^{-1}, which is significantly higher than that of conventional SPR metal-ion sensors reported in earlier studies [13,14,19].

In the similar way, Fig. 6 and Fig. 7 have been plotted for different concentrations of Pb^{2+} ions [Table 2].

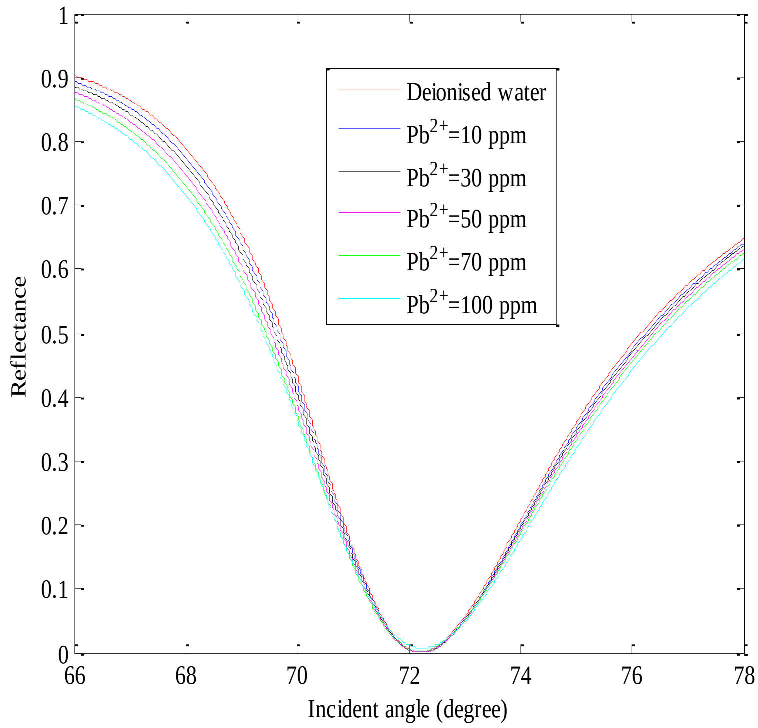

Fig. 6. At optimized thickness of Au, the reflectivity curve is plotted for different concentration 0 to 100 ppm of Pb^{2+} metal ion.

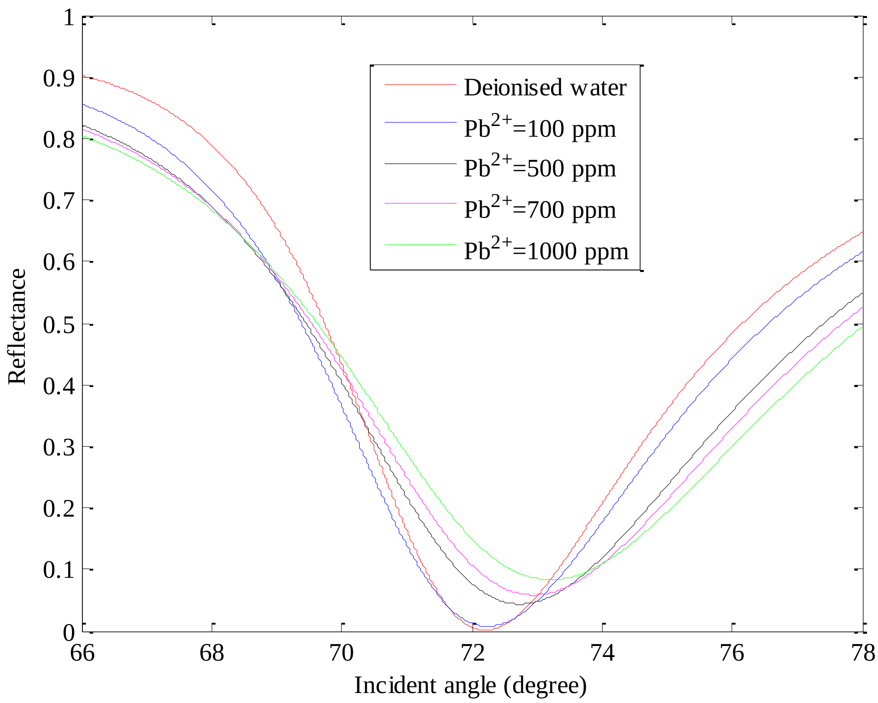

Fig. 7. At optimized thickness of Au, the reflectivity curve is plotted for different concentration 100 to 1000 ppm of Pb^{2+} metal ion.

From Fig. 6, it is evident that the resonance angle shows no noticeable change for low Pb^{2+} concentrations ranging from 0 ppm to 100 ppm. This may occur due to similar value of refractive index of low concentration Pb^{2+} ions as happened in case of Hg^{2+} ion. In Fig. 7, the resonance angle changes very significantly for various concentrations of Pb^{2+} ions (i.e. 100 ppm to 1000 ppm). The obtained resonance angle for 100 ppm, 500 ppm, 700 ppm and 1000 ppm is 72.25^0, 72.75^0, 72.96^0

and 73.21^0 respectively. From Fig. 7 and using the Eq. (9), the calculated value of sensitivity comes out to be 139.43^0/RIU which is also greater than the conventional SPR metal ion sensor [13,14,19].

This enhancement in sensitivity may arise due to the presence of high refractive index material i.e. $BaTiO_3$. Applying this high refractive index layer to the prism base effectively improves the performance of the SPR metal-ion sensor.

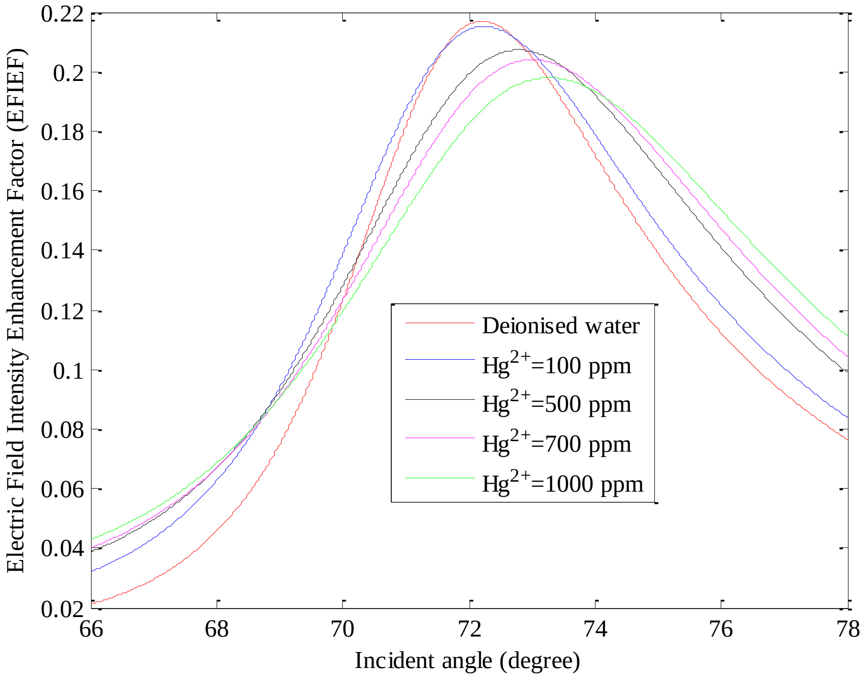

Fig. 8. Electric Field Intensity Enhancement plot for Hg^{2+} ions.

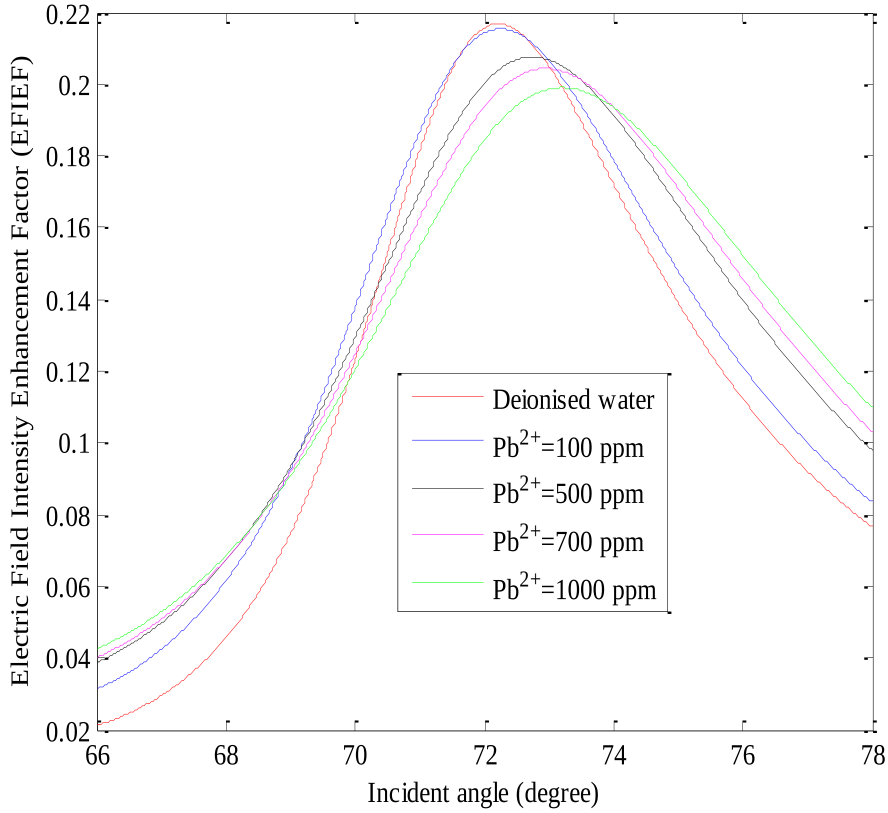

Fig. 9. Electric Field Intensity Enhancement plot for Pb^{2+} ions.

Fig. 8 and 9 is the plot of EFIEF. In both Fig. 8 and Fig. 9, the EFIEF has been found to be maximum at the respective resonance angles for both metal ions i.e. $Hg^{2+}$and Pb^{2+}. As the metal-ion concentration rises, the electric field strength gradually decreases because a higher number of ions accumulate at the sensing surface, reducing the overall field intensity.

Finally, Fig. 10 has been plotted between reflectance and resonance angle for different concentrations of both the metal ions.

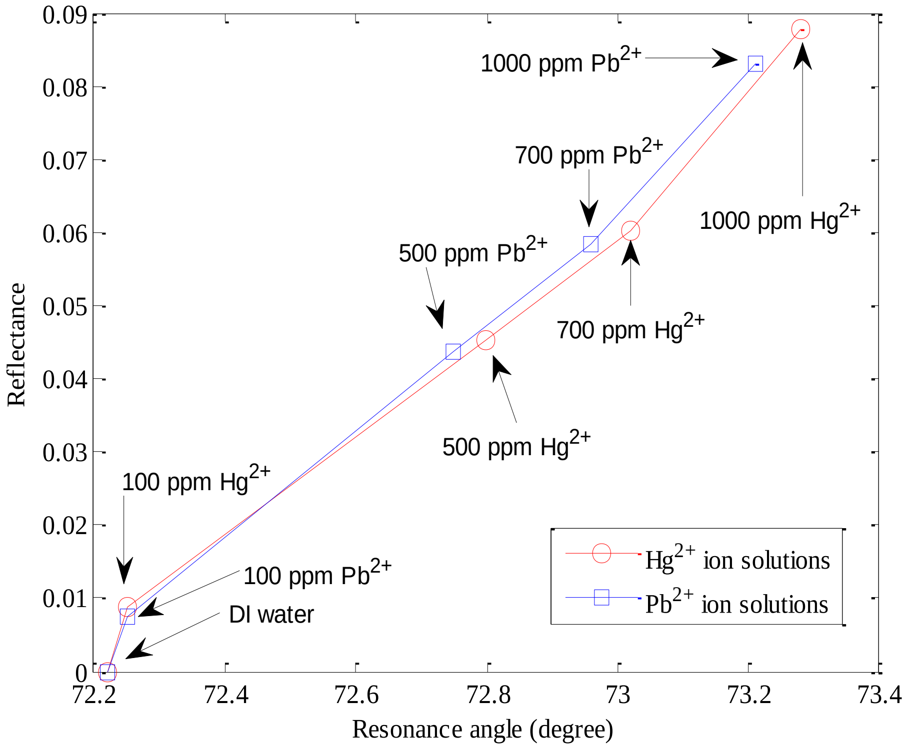

Fig. 10. Reflectance versus resonance angle plot for different concentrations of Hg^{2+} and Pb^{2+} metal ions.

It is clear from Fig. 10, for the concentration 100 ppm both the metal ion solutions have the same resonance angle which occurs due to their similar refractive indices for very small concentration. As the concentration changes, the refractive index differs and hence the resonance angle changes. The reflectance corresponding to different concentrations of Hg^{2+}metal ion 100 ppm to 1000 ppm at resonance angle 72.220, 72.25^0, 72.80^0, 73.02^0 and $73.28^0$is found to be 0.0087, 0.0452, 0.0603 and 0.0879 respectively. Also, the reflectance corresponding to different concentrations of Pb^{2+}metal ion 100 ppm to 1000 ppm at resonance angle 72.25^0, 72.75^0, 72.96^0 and $73.21^0$is found to be 0.0074, 0.0436, 0.0583 and 0.08307 respectively.

A similar reflectance pattern is observed for both metal ions due to their closely matched refractive indices, which result from their small size difference and adjacent positions in the periodic table.

From the above discussion, it is evident that the proposed SPR metal-ion sensor exhibits higher sensitivity compared to conventional SPR sensors, highlighting its potential technological significance in various sensing applications. A comparison of the results from the present study with previously reported conventional sensors is summarized in Table 4.

Table 4.3 Sensitivity comparison of proposed and reported SPR metal-ion sensors

S. No.	Metal ions	Sensitivity (deg/RIU)	Reference
1	Pb^{+2} Hg^{+2}	74.32 74.64	[19]
2	Pb^{+2}	70.50	[14]
3	Pb^{+2} Hg^{+2}	11.98 5.83	[13]
4	Pb^{+2} Hg^{+2}	139.43 141.00	present study

Conclusions:

In this study, we show the advantage of adding a high-dielectric material at the base of the prism for detecting heavy metal ions. The results of the proposed sensor, along with previous conventional sensors, are shown in Table 4. By coating a thin layer of $BaTiO_3$, the performance of the SPR metal-ion sensor is significantly improved. For Hg^{2+} detection, the sensitivity (S), detection accuracy (DA), and quality parameter (QP) are 1410 RIU^{-1}, 0.178, and 23.77 RIU^{-1}. For Pb^{2+} detection, these values are 1390.43 RIU^{-1}, 0.166, and 23.51 RIU^{-1}, all higher than earlier reported sensors.

Acknowledgement
Dr. Angad Singh Kushwaha and Dr. Rajeev Kumar are grateful to their institutions for providing good platform to carry out this research work.

Financial support and sponsorship
Nil.

Conflicts of interest
The authors declare that there are no conflicts of interest regarding the publication of this paper.

References:

1. B.K. Bansod, T. Kumar, R. Thakur, S. Rana, I. Singh, A review on various electrochemical techniques for heavy metal ions detection with different sensing platforms, Biosensors and Bioelectronics 94 (2017) 443–455.
2. T.W. Clarkson, L. Magos, G.J. Myers, The toxicology of mercury-Current exposures and clinical manifestation, N Engl. J Med. 349 (2003) 1731-1737.
3. R. A. Goyer, Lead toxicity: From overt to subclinical to subtle health effects, Environ. Health Perspect. 86(1990) 177-181.
4. R. R. Dietert,E. Lee, I. Hussain, M. Piepenbrink, Developmental immune toxicology of lead, Toxicol. Appl. Pharracol 198 (2004) 86- 94.
5. S. Wang, E. S. Forzani N. Tao, Detection of heavy metal ion in water by high-resolution surface plasmon resonance spectroscopy combined with anodic stripping voltammetry, Anal. Chem. 79 (2007) 4427-4432.
6. Y. M. Panta, Liu, M. A. Cheney, S. W, S. Qia, Ultrasensitive detection of mercury (II) ions using electrochemical surface plasmon resonance with magneto hydrodynamic convection, J Colloid Inter. Sci. 333 (2009) 485-490.
7. K. Fahnestock, M. Manesse, H. A. McIiwee, C. L. Schauer, R. Boukherroub, S. Szunerits, Selective detection of hexachromium ions by localized surface plasmon resonance measurements using gold nanoparticles/chitosan composite interfaces, Analyst 134 (2009) 881-886.
8. L. Wang, T. Li, Y. Du, C. Chen, B. Li, M. Zhou, S. Dong, Au NPs enhanced surface plasmon resonance for sensitive detection of mercury (II) ions, Biosens. Bioelectron. 25 (2010) 2622-2626.
9. J. Homola, S.S. Yee, G. Gauglitz, Surface plasmon resonance sensors: review, Sens. Actuators B 54 (1999) 3–15.
10. H. Reather, Surface plasmons on smooth and rough surfaces and on gratings, Springer Tracts in Modern Physics, Springer Verlag 1988.
11. K. Ock, G. lag, Y. Roh, S. Kim, Kim, K. Koh, Optical detection of Cu2+ ion using a SQ-dye containing polymeric thin-film on Au surface, Microcher. J. 70 (2001)301-305.
12. S. W. Chah, H. Yi, R. N. Zare, Surface plasmon resonance analysis of aqueous mercuric ions, Sens. Actuators B: Chem. 99(2004) 216-222.
13. W. M. Mukhtar, R. M. Halim, K. A. Dasuki, A. Rozana, A. Rashid, N. Athirah, M. Taib, SPR sensor for detection of heavy metal ions: Manipulating the EM waves polarization modes, Malaysian Journal of Fundamental and Applied Sciences 13 4 (2017) 619-622.
14. Y. Wing, W. Fen, M. M. Yunus, Z. A. Talib, Analysis of Pb(II) ion sensing by crosslinked chitosan thin film using surface plasmon resonance spectroscopy, Optik 124 (2013) 126–133.
15. Y. Wang, W. Chen, B. Wang, Y. Zheng, Ultrathin Ferroelectric Films: Growth, Characterization, Physics and Applications, Materials 7(9) (2014) 6377-6485.
16. A. Petraru, J. Schubert, M. Schmid, Ch. Buchal, Ferroelectric BaTiO3 thin-film optical waveguide modulators, Appl. Phys. Letts. 81 (2002) 8.
17. P. Tang, D. J. Towner, T. Hamano, A. L. Meier, B. W. Wessels, Electrooptic modulation up to 40 GHz in a barium titanate thin film waveguide modulator, Optics Express 12 (2004) 5962-5967.
18. M J. Dicken, L A. Sweatlock, D Pacifici, H J. Lezec, K Bhattacharya, H A. Atwater, Electrooptic modulation in thin film barium titanate plasmonic interferometer, Nano letters. 8 (2008) 11 4048-4052.
19. Y. W. Fen, W. M. M. Yunus, Characterization of the optical properties of heavy metal ions using surface plasmon resonance technique, Optics and Photonics Journal,1 (2011) 116-123.
20. R. Kumar, A.S. Kushwaha, M. Srivastava, H. Mishra, S.K. Srivastava, Enhancement in sensitivity of graphene-based zinc oxide assisted bimetallic surface plasmon resonance (SPR) biosensor, Appl. Phys. A 124 (2018) 235.
21. Angad S. Kushwaha, Anil Kumar, Rajeev Kumar, S.K. Srivastava, A study of surface plasmon resonance (SPR) based biosensor with improved sensitivity, Photon. Nanostruct. Fundam. Appl. 31 (2018) 99–106.
22. Angad S. Kushwaha, Anil Kumar, Rajeev Kumar, Monika Srivastava, S.K. Srivastava, Zinc oxide, gold and graphene-based surface plasmon resonance (SPR) biosensor for detection of pseudomonas like bacteria: A comparative study, Optik 172 (2018) 697–707.
23. M. Yamamoto, Surface plasmon resonance (SPR) theory: tutorial, Rev. Polarogr. 48 (2002) 209.